# Vascular endothelial growth factor selectively targets boronated dendrimers to tumor vasculature

**Marina V. Backer,[1] Timur I. Gaynutdinov,[1] Vimal Patel,[1] Achintya K. Bandyopadhyaya,[2] B.T.S. Thirumamagal,[2] Werner Tjarks,[2] Rolf F. Barth,[3] Kevin Claffey,[4] and Joseph M. Backer[1]**

[1]SibTech, Inc., Newington, Connecticut; [2]College of Pharmacy and [3]Department of Pathology, The Ohio State University, Columbus, Ohio; and [4]University of Connecticut, Health Center, Farmington, Connecticut

## Abstract

**Tumor neovasculature is a potential but, until very recently, unexplored target for boron neutron capture therapy (BNCT) of cancer. In the present report, we describe the construction of a vascular endothelial growth factor (VEGF)–containing bioconjugate that potentially could be used to target up-regulated VEGF receptors (VEGFR), which are overexpressed on tumor neovasculature. A fifth-generation polyamidoamine dendrimer containing 128 reactive amino groups was reacted with 105 to 110 decaborate molecules to produce a macromolecule with 1,050 to 1,100 boron atoms per dendrimer. This was conjugated to thiol groups of VEGF at a 4:1 molar ratio using the heterobifunctional reagent sulfo-LC-SPDP. In addition, the boronated dendrimer was tagged with a near-IR Cy5 dye to allow for near-IR fluorescent imaging of the bioconjugate *in vitro* and *in vivo*. As would be predicted, the resulting VEGF-BD/Cy5 bioconjugate was not cytotoxic to HEK293 cells engineered to express $2.5 \times 10^6$ VEGFR-2 per cell. Furthermore, it showed binding and activation of VEGFR-2 comparable with that of native VEGF. Internalization of VEGF-BD/Cy5 by PAE cells expressing $2.5 \times 10^5$ VEGFR-2 per cell was inhibited by excess VEGF, indicating a VEGFR-2-mediated mechanism of uptake. Near-IR fluorescent imaging of 4T1 mouse breast carcinoma revealed selective accumulation of VEGF-BD/Cy5, but not BD/Cy5, particularly at the tumor periphery where angiogenesis was most active. Accumulation of VEGF-BD/Cy5 in 4T1 breast carcinoma was diminished in mice pretreated with a toxin-VEGF fusion protein that selectively killed VEGFR-2-overexpressing endothelial cells. Our data lay the groundwork for future studies using the VEGF-BD/Cy5 bioconjugate as a targeting agent for BNCT of tumor neovasculature. [Mol Cancer Ther 2005;4(9):1423–9]**

## Introduction

Boron neutron capture therapy (BNCT) is based on the selective delivery of boron-10 ($^{10}B$) to tumor cells (1, 2). Following irradiation with low-energy neutrons, nuclear capture and fission reactions occur that produce $He^{2+}$ and $Li^{3+}$ particles. These high linear energy transfer particles can travel only 5 to 10 μm from the site of their origin and therefore are lethal only to those cells that bind or internalize $^{10}B$ in sufficient concentrations. It was thought that the effects of BNCT were based solely on its ability to produce double-stranded DNA breaks. The effectiveness of BNCT is dependent upon the amount of $^{10}B$ deliver per cell. Approximately $10^9$ $^{10}B$ atoms per tumor cell are necessary to produce four to five α particles per cell (3), but studies of radiation-induced apoptosis suggest that BNCT also may be cytotoxic via other mechanisms (4) so that the required number of $^{10}B$ atoms actually may be less. Nevertheless, this requirement has been the driving force for the development of high-capacity targeted boron carriers, such as epidermal growth factor and monoclonal antibodies, to selectively deliver large numbers of boron atoms to the target tumor (5–9). A common approach has been to use decaborate clusters either alone or attached to high-capacity carriers such as polyamidoamine (PAMAM or ''starburst'') dendrimers. These macromolecules have large numbers of amino groups that can be linked to receptor-specific targeting agents. The use of decaborate-substituted fourth- or fifth-generation PAMAM dendrimers, or other high-capacity carriers, conjugated to epidermal growth factor (7, 10–12), monoclonal antibodies (13, 14), or bispecific antibodies (15, 16) to target brain tumors, or folic acid (17) to target other tumor types have been described. Convection-enhanced delivery was used to improve intracerebral accumulation of these high molecular weight agents while decreasing their uptake by extracranial organs (5, 9). However, these boron-containing conjugates encounter the same problem as any other antitumor biologicals; that is, they are removed from the bloodstream faster than they can be selectively delivered to tumor cells across the vascular endothelial cell barrier. Development of pegylated boron-containing bioconjugates with longer circulation times is one approach that might alleviate this problem (17).

Received 5/18/05; revised 6/30/05; accepted 7/15/05.

**Grant support:** Department of Energy grant DE-FG-2-02ER83520 (J.M. Backer) and NIH grant 1R01 CA098945 (R.F. Barth).

The costs of publication of this article were defrayed in part by the payment of page charges. This article must therefore be hereby marked advertisement in accordance with 18 U.S.C. Section 1734 solely to indicate this fact.

**Requests for reprints:** Marina V. Backer, Sibtech, Inc., 705 North Mountain Road, Newington, CT 06111. Phone: 860-953-1164; Fax: 860-953-1317. E-mail: mbacker@sibtech.com



doi:10.1158/1535-7163.MCT-05-0161

An alternative approach would be to target endothelial cells of the tumor vasculature rather than the tumor itself. The growth of primary tumor and metastatic lesions beyond a few millimeters depends on the development of new blood vessels (neovascularization) via a tightly controlled process known as angiogenesis (18). The crucial positive regulator of angiogenesis is vascular endothelial growth factor (VEGF), which is a secreted dimeric glycoprotein whose action on endothelial cells is mediated mostly by VEGFR-2 (KDR/Flk-1) tyrosine kinase receptor (19). Endothelial cells in tumor neovasculature express significantly greater numbers of VEGFR-2 than quiescent endothelial cells (20, 21). In addition, in some tumors VEGFR-2 expression was also detected on tumor cells (22, 23). This provides a unique opportunity to selectively target VEGFR-2-overexpressing cells with VEGF-driven cytotoxic or cytostatic constructs (24–26).

In the present report, we describe the synthesis of a VEGF-driven boronated dendrimer using human recombinant $VEGF_{121}$, expressed as a fusion protein with a novel cysteine-containing peptide fusion tag, and a fifth-generation of PAMAM dendrimer containing 128 primary amino groups, which has been linked to 105 to 110 decaborate molecules. To facilitate *in vivo* analysis, these dendrimers also were labeled with a near-IR dye Cy5, for near-IR fluorescent imaging of their biodistribution and uptake in tumor-bearing mice. The VEGF-driven boronated dendrimers retained the functional activities of VEGF, were internalized by cells via receptor-mediated endocytosis, and were neither cytotoxic nor growth promoting *in vitro* for cells overexpressing VEGFR-2. Furthermore, *in vivo* near-IR fluorescent imaging studies revealed that these bioconjugates accumulated in tumor vasculature and that their uptake was mediated by VEGFR-2-positive cells.

## Materials and Methods

### Materials

A fifth-generation PAMAM dendrimer containing 128 reactive amino groups (G5) was from Sigma-Aldrich Corp. (St. Louis, MO). $Na(CH_3)_3NB_{10}H_8NCO$ was prepared from $(CH_3)_3NB_{10}H_8CO$ (Katchem Ltd., Prague, Czech Republic), as described (27). Sulfosuccinimidyl 6-[3′ (2-pyridyldithio)-propionamido]hexanoate (Sulfo-LC-SPDP) and *N*-hydroxysuccinimidyl (NHS) acetate were from Pierce (Rockford, IL). Cy5-NHS and PD-10 disposable desalting columns were from Amersham Pharmacia Biotech (Piscataway, NJ). 3-(1-Methylpiperidinium)-1-propane sulfonate (NDSB-221) was from Novagen (Madison, WI).

### Derivatization of G5 Dendrimers with Near-IR Cy5 Dye and Bifunctional Cross-Linking Reagent Sulfo-LC-SPDP

G5 dendrimer (0.5 μmol in methanol), Cy5-NHS (0.6 μmol in dimethylformamide), and Sulfo-LC-SPDP (0.8 μmol in dimethylformamide) were mixed and incubated for 1 hour, diluted 2.2-fold with 20 mmol/L carbonate buffer (pH 9.0), and desalted on a PD-10 column. Concentration of Cy5 residues in the intermediate product Cy5/SPDP-G5 was determined using Cy5 extinction coefficient $\varepsilon_{650}$ = 250,000 $(mol/L)^{-1}$ $cm^{-1}$ (28). SPDP concentration was determined by complete oxidation with 10 mmol/L DTT for 1 hour at 37°C and subsequent measuring the concentration of released pyridine-2-thione [$\varepsilon_{343}$ = 8,080 $(mol/L)^{-1}$ $cm^{-1}$].

### Derivatization of Cy5/SPDP-G5 with $Na(CH_3)_3NB_{10}H_8NCO$

Modification of Cy5/SPDP-G5 with $Na(CH_3)_3NB_{10}H_8NCO$ was done as described (14), with modifications. Briefly, Cy5/SPDP-G5 (0.31 μmol in carbonate buffer) was mixed with $Na(CH_3)_3$-$NB_{10}H_8NCO$ (100 μmol in acetone) and incubated for 24 hours to yield Cy5/SPDP-G5-B. The remaining amino groups in Cy5/SPDP-G5 were blocked by incubation with NHS acetate (65.6 μmol) for 1 hour. The precipitate formed during incubation was collected by centrifugation, dissolved in DMSO, diluted 1:4 with 20 mmol/L Tris-HCl (pH 8.0), and precipitated with 0.25 volume of 5 mol/L NaCl. The pellet was dissolved in 20 mmol/L Tris-HCl (pH 8.0) and desalted. The concentration of boronated dendrimers (i.e., BD/Cy5) was determined by measuring Cy5 and SPDP concentrations as described above. Boron content, equal to 105 to 110 dodedecaborate molecules (or 1,050–1,100 boron atoms) per dendrimer, was determined using a Perkin-Elmer Optima 4300DV inductively coupled plasma optical emission spectrometer. A measured amount of dendrimer in buffer (NaPi/NaCl/DMSO, pH 7.2) was digested using an Ethos 320 microwave autoclave (Milestone, Inc., Durham, NC), redissolved in 5% $HNO_3$, and used as a sample for inductively coupled plasma optical emission spectrometer measurement. Five standard solutions of boron (Certiprep, CPI International, Santa Rosa, CA) were used to generate a calibration curve, and the boron content of the samples was calculated automatically with the WinLab32 software.

### Conjugation of Boronated Dendrimers to VEGF

A 121-amino-acid isoform of human VEGF with $NH_2$-terminal Hu-tag (a 1–15-amino-acid fragment of human RNase I) fused via a $(G_4S)_3$ linker was constructed as described (29). Cysteine at position 4 of Hu-tag was introduced by site-directed mutagenesis using Gene-Tailor Site Directed mutagenesis kit (Invitrogen, Carlsbad, CA). To obtain free SH groups, VEGF was incubated with a 1.5-fold molar excess DTT in 0.1 mol/L Tris-HCL (pH 8.0), 0.5 mol/L urea, and 0.5 mol/L NDSB-221 for 16 hours at 4°C and desalted. Free SH-groups were detected by reacting them with *N*-(1-pyrene)-maleimide (Molecular Probes, Eugene, OR), as described (30, 31). Desalted protein was mixed with BD/Cy5 at a molar ratio of 1:2 and, after a 15-minute incubation, the resulting bioconjugate VEGF-BD/Cy5 was precipitated twice with 0.25 volume of 5 mol/L NaCl, spun down by centrifugation, and redissolved in 20 mmol/L Tris-HCl (pH 8.0). The molar ratio of VEGF to BD/Cy5 in the purified bioconjugate was determined via its cleavage with 10 mmol/L DTT for 1 minute at 95°C followed by reverse-phase high-performance liquid chromatography analysis of the products on a C4 Vydac column.

### Cells

HEK293 human transformed embryonic kidney cells (CRL-1573) and 4T1 mouse breast carcinoma cells (CRL-2539) were from the American Type Culture Collection (Manassas, VA). 293/KDR cells expressing $2.5 \times 10^6$ VEGFR-2 per cell were described elsewhere (32). PAE porcine aortal endothelial cells expressing $2 \times 10^5$ VEGFR-2 per cell (PAE/KDR) were kindly provided by Dr. B. Terman (Albert Einstein School of Medicine, Bronx, NY). All cells were grown in DMEM with 10% fetal bovine serum, 2 mmo/L L-glutamine, and antibiotics at 37°C in 5% $CO_2$.

### VEGFR-2 Autophosphorylation

293/KDR cells were plated into 24-well plates ($7.5 \times 10^4$ cells per well), shifted to starvation medium (DMEM/0.5% fetal bovine serum) 6 hours later, and incubated for 16 hours at 37°C in 5% $CO_2$. Then cells were switched to serum-free DMEM with 0.5 mmol/L sodium vanadate for 20 minutes at 37°C, stimulated with VEGF or VEGF-BD/Cy5 for 10 minutes at 37°C, lysed, and analyzed by Western blotting using anti-phosphotyrosine RC20 antibody conjugated to horse radish peroxidase (BD Transduction Laboratories, San Diego, CA).

### SLT-VEGF Protection Assay

SLT-VEGF fusion toxin ($VEGF_{121}$ fused to the Shiga-like toxin subunit A) was expressed as described (25). The SLT-VEGF protection assay was done as described (33). Briefly, 293/KDR cells were plated on 96-well plates (1,000 cells per well). Varying amounts of VEGF-BD/Cy5 were mixed with SLT-VEGF in complete culture medium and added to cells in triplicate wells to a final SLT-VEGF concentration of 1 nmol/L. Cells were quantitated 96 hours later by CellTiter 96 $AQ_{ueous}$ One Solution Cell Proliferation Assay kit (Promega, Madison, WI).

### Confocal Microscopy

PAE/KDR cells were plated on glass coverslips (20,000 cells per coverslip), switched to starvation medium 6 hours later, and incubated for 16 hours at 37°C in 5% $CO_2$. VEGF-BD/Cy5 was added to cells to a final concentration of 14 nmol/L VEGF either alone, or as a mixture with a 100-fold molar excess of VEGF. BD/Cy5 was added to control cells to a final Cy5 concentration of 20 nmol/L. After a 15-minute incubation at 37°C, medium was aspirated and cells were washed twice with PBS and once with 0.4 mol/L NaCl/PBS. After a 5-minute fixation in fresh 4% formaldehyde, cells were washed twice with PBS and once with deionized water. Coverslips were mounted on slides in the mounting medium for fluorescence microscopy (Vector Laboratories, Burlingame, CA) and examined with a confocal microscope using a 630× magnification. Images were transferred to Adobe Photoshop (version 6.0), combined, and the tonal range of the image grayscale was adjusted to increase the contrast (Adobe command: Image > Adjust > Auto level).

### Optical Imaging of VEGF-BD/Cy5 *In vivo*

Female, 5- to 6-week-old BALB/c mice were from Charles River Laboratories (Wilmington, MA). 4T1 breast carcinoma cells were implanted s.c. in the dorsum of mice ($5 \times 10^3$ cells per mouse). VEGF-BD/Cy5 was injected in the tail vein on the 13th day after tumor implantation. Animals were anesthetized 5 minutes after VEGF-BD/Cy5 injections and imaged using Kodak Image Station 2000 Multi-Modal Imaging System (IS2000 MM) using 625- and 700-nm filters for excitation and emission light, respectively. Kodak Image Analysis Software was used to convert images to ''fire'' pseudocolor and for analysis of image regions of interest. The protocol for the animal studies was reviewed and approved by the Institutional Animal Care and Use Committee at the University of Connecticut Health Center.

## Results

### Synthesis of VEGF-BD/Cy5

Multifunctional conjugates were synthesized through several steps (Fig. 1). First, using Cy5-NHS, the G5 dendrimers were derivatized with a near-IR dye Cy5, to a molar ratio of one molecule of Cy5 per dendrimer. Simultaneously, the dendrimers were derivatized with the bifunctional cross-linking agent sulfo-LC-SPDP at a molar ratio of one sulfo-LC-SPDP per dendrimer yielding Cy5/SPDP-G5. Derivatization of Cy5/SPDP-G5 with

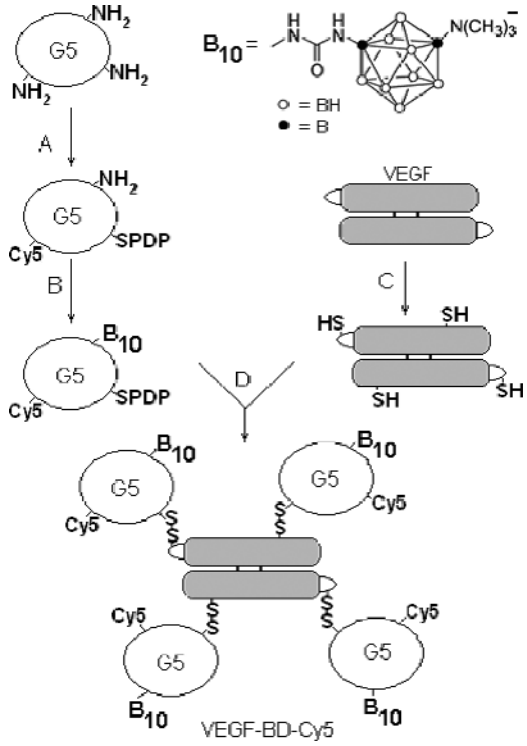


**Figure 1.** Synthesis of VEGF-BD/Cy5. **A,** G5 (fifth-generation PAMAM dendrimer) was incubated with SPDP and Cy5-NHS, 20.5% dimethylformamide in methanol for 1 h. **B,** reaction with $Na(CH3)_3$-$NB_{10}H_8NCO$ in 20 mmol/L carbonate buffer (pH 9.0)/9% acetone for 24 h. **C,** 1.5-fold molar excess DTT over a VEGF monomer in 20 mmol/L NaOAc (pH 6.5), 0.5 mol/L urea, 0.5 mol/L NDSB-221 at 4°C for 16 h. **D,** conjugation in 20 mmol/L Tris-HCl (pH 8.0) for 15 min.

$Na(CH_3)_3NB_{10}H_8NCO$ clusters yielded BD/Cy5 constructs (Fig. 1) containing 105 to 110 boron clusters (1,050–1,100 boron atoms) per dendrimer. These results indicate that the majority of the 126 available amino groups of BD/Cy5 were derivatized with the decaborate clusters.

To generate thiol groups available for cross-linking, VEGF (a 121-amino-acid isoform with a cysteine containing Hu-tag), containing 20 cysteine residues per dimer, was treated with DTT under mild denaturing conditions yielding partially reduced VEGF with two thiol groups available for cross-linking, as determined by the reaction with *N*-(1-pyrene)-maleimide (31, 32). Our preliminary results indicate that the cysteine residues C4 in the $NH_2$-terminal tag and C116 (position −5 at VEGF COOH terminus) may have become available for cross-linking under the selected reducing conditions.[5] BD/Cy5 was conjugated to partially reduced VEGF via sulfhydryl exchange, yielding VEGF-BD/Cy5 with four boronated dendrimers per VEGF dimer. This ratio was determined by high-performance liquid chromatography analysis of the purified conjugates under reducing conditions that released VEGF (Fig. 2).

### Functional Activities of VEGF-BD/Cy5

The targeted boronated dendrimers might be cytotoxic via a variety of mechanisms. Therefore, we tested how VEGF-BD/Cy5 might affect the growth of 293/KDR cells. These cells showed small but significant growth stimulation when exposed to Hu-tagged $VEGF_{121}$ but not VEGF-BD/Cy5 (Fig. 3A). However, there was no growth inhibition until a nonphysiologic concentration of 200 nmol/L of VEGF-BD/Cy5 was added to the culture. To determine how modification of VEGF with boronated dendrimers affected its functional activity, we used two assays with different time spans. In a short-term assay, VEGF-BD/Cy5 was tested for its ability to induce tyrosine autophosphorylation of VEGFR-2 in 293/KDR cells. As shown in Fig. 3B, activity of VEGF-BD/Cy5 was similar to that of VEGF in the concentration range of 0.8 to 4 nmol/L, although at lower concentrations, VEGF-BD/Cy5 was slightly less effective than VEGF. In the long-term assay, VEGF-BD/Cy5 was tested for its ability to protect 293/KDR cells from cytotoxicity of SLT-VEGF fusion toxin (25). Although 293/KDR cells are very sensitive to SLT-VEGF ($IC_{50}$ < 0.1 nmol/L), they can be rescued in a dose-dependent manner by VEGF (Fig. 3C). In this assay, VEGF-BD/Cy5 was marginally less effective than VEGF (Fig. 3C). Taken together, both short- and long-term assays indicated that the modification of the $VEGF_{121}$ dimer with four boronated dendrimers only minimally affected the ability of VEGF to interact with and activate VEGFR-2.

### Receptor-Mediated Internalization of VEGF-BD/Cy5

Because the high linear energy transfer particles produced as a result of the $^{10}B(n,\alpha)^7Li$ capture reaction have a path length of only 5 to 10 μm, it was important to establish whether VEGF-BD/Cy5 was internalized via receptor-mediated endocytosis. We therefore evaluated internalization of VEGF-BD/Cy5 in PAE/KDR cells ($2 \times 10^5$ VEGFR-2 per cell) with confocal fluorescence microscopy. VEGF-BD/Cy5 was internalized and localized mostly in the perinuclear region with a distinct punctate pattern (Fig. 4A). Internalization was receptor mediated, because incubation of cells with a mixture of VEGF-BD/Cy5 and unlabeled VEGF resulted in a ~10-fold decrease in the total amount of Cy5 signal (Fig. 4B) as estimated by quantitative analysis of confocal images with the same exposure conditions, using Adobe Photoshop command ''Image > Histogram'' to determine the numbers of white pixels corresponding to the Cy5 signal. Interestingly, untargeted BD/Cy5 also was internalized by PAE/KDR cells (Fig. 4C). However, the pattern of intracellular distribution was distinct from that of VEGF-BD/Cy5, because it was found mostly in the nucleus as rather large ''spots'' and diffuse staining on cell membranes and cytoplasm.

### Near-IR Fluorescent Imaging of Tumor Vasculature with VEGF-BD/Cy5

Although VEGF-BD/Cy5 retained its ability to bind, activate, and internalize VEGFR-2 in tissue culture, it was crucial to establish its activity *in vivo*. Because

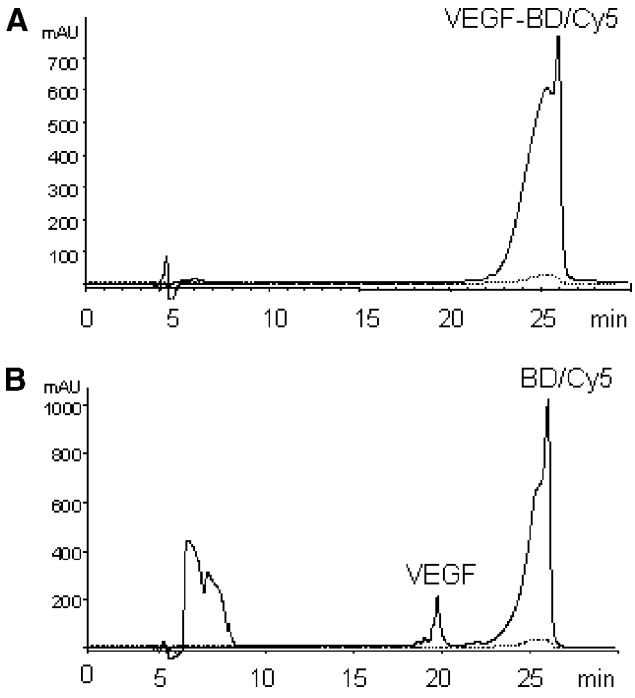


**Figure 2.** VEGF-BD/Cy5 conjugate releases VEGF under reducing conditions. **A**, VEGF-BD/Cy5 was analyzed by reverse-phase high-performance liquid chromatography on Vydac Protein C4 (214TP54) column (250 × 4.6 mm) with an elution rate of 0.75 mL/min with 0.1% aqueous trifluoroacetic acid/acetonitrile gradient (5–95% over 30 min) and detection at 216 nm (*solid line*) and 600 nm (*dashed line*). **B**, VEGF-BD/Cy5 was treated with 10 mmol/L DTT at 95°C for 1 min before reverse-phase high-performance liquid chromatography analysis. Molar VEGF to BD/Cy5 ratio was calculated as the ratio of the integral intensity of the peaks corresponding to VEGF and BD/Cy5. Note that absorption at 600 nm corresponding to Cy5 overlaps with the BD/Cy5 peak after DTT treatment. The peak between 5 and 8 min is of systemic origin.

[5] M.V. Backer, unpublished.

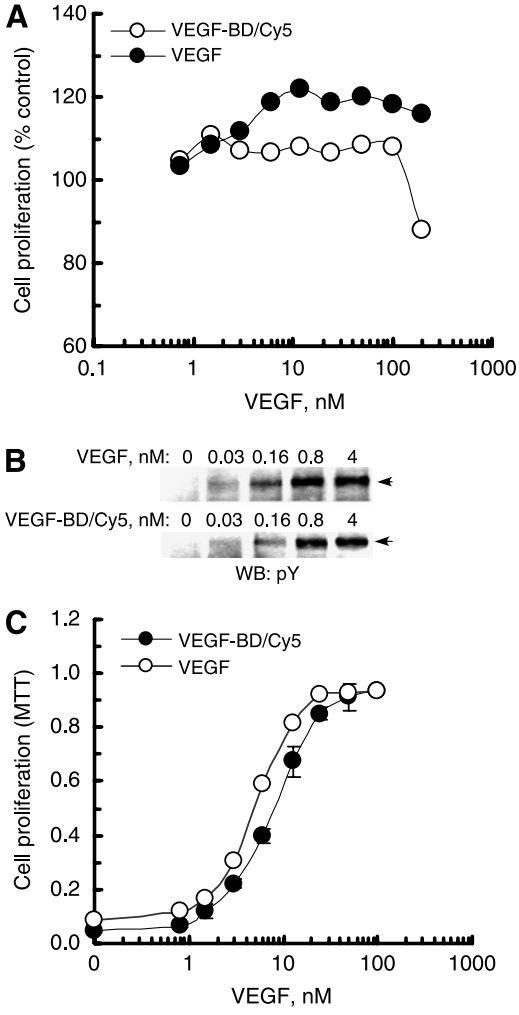


**Figure 3.** Testing VEGF-BD/Cy5 in tissue culture. **A**, VEGF-BD/Cy5 is not cytotoxic for 293/KDR at physiologic concentrations. 293/KDR cells were plated on 96-well plates (1,000 cells per well). Varying amounts of VEGF or VEGF-BD/Cy5 were added to cells in triplicate wells to indicated final concentrations. Cells were quantitated 96 h later by CellTiter 96 $AQ_{ueous}$ One Solution Cell Proliferation assay. **B**, VEGF-BD/Cy5 induces VEGFR-2 tyrosine autophosphorylation. 293/KDR cells were stimulated with indicated concentrations of VEGF or VEGF-BD/Cy5 for 10 min at 37°C, lysed, and analyzed by Western blotting. Arrows indicate positions of VEGFR-2. **C**, VEGF-BD/Cy5 protects 293/KDR cells from SLT-VEGF cytotoxicity. VEGF-BD/Cy5 or VEGF were mixed with SLT-VEGF in complete culture medium to a final SLT-VEGF concentration of 1 nmol/L, added to cells in triplicate wells, and quantitated 96 h later.

VEGF-BD/Cy5 was designed to serve as a diagnostic tool as well as a potential therapeutic agent, we tested its ability to image tumor vasculature. VEGF-BD/Cy5 injected i.v. selectively accumulated in areas at the edge of growing s.c. 4T1 tumors where active angiogenesis takes place and, presumably, neovasculature is enriched with endothelial cells overexpressing VEGFR-2 (Fig. 5A). Quantitative analysis of the regions of interest indicated that the amount of accumulated VEGF-BD/Cy5 increased steadily over ~1 hour until reaching a stable plateau, which lasted for at least 2 hours (data not shown).

The selective accumulation of VEGF-BD/Cy5 was not due to enhanced permeability of the tumor vasculature, because treatment with BD/Cy5 control resulted in a barely detected Cy5 signal in the tumor area (Fig. 5B). The significance of VEGF-dependent accumulation was further evident in experiments with tumor-bearing mice that were systemically treated with SLT-VEGF. The latter treatment dramatically decreased the number of VEGFR-2-positive cells in 4T1 tumors.[6] We found that s.c. injections of SLT-VEGF (1 μg per mouse) on days 4 and 7 after tumor implantation before near-IR fluorescent imaging on day 13 decreased the selective accumulation of VEGF-BD/Cy5 by ~10-fold (Fig. 5C–D).

## Discussion

Targeting tumor vasculature in addition to tumor cells could be a useful way to enhance the efficacy of BNCT. Because endothelial cells in tumor neovasculature overexpress VEGFR, particularly VEGFR-2, the use of VEGF as a boron delivery agent might be an effective antiangiogenic strategy. Exploring this approach, Koning et al. recently have reported on the targeting of human umbilical vein endothelial cells with integrin-specific RGD peptides coupled to liposomes that contained disodium dodecahydrodocaborate (34). Specific localization to the perinuclear region of human umbilical vascular endothelial cell was shown *in vitro* by means of confocal laser scanning microscopy. Following neutron irradiation, there was a 2-fold reduction in cell viability compared with control with nontargeted liposomes. Based on these studies, the authors propose to use the RGD liposomes for targeting tumor vasculature. In the present report, we have described the production and evaluation of VEGF-BD/Cy5, a functionally active VEGF dimer containing four boronated fifth-generation PAMAM dendrimers with a total ''payload'' of 4,200 to 4,400 boron atoms. Boronated dendrimers were derivatized with the heterobifunctional cross-linking reagent sulfo-LC-SPDP for conjugation to VEGF cysteine residues and tagged with a near-IR fluorochrome (Cy5) dye for near-IR fluorescent imaging of the conjugates *in vitro* and *in vivo*. Because the overall molecular weight of a fully modified dendrimer is ~56,000 kDa, conjugation of four dendrimers to a ~33 kDa VEGF yielded a conjugate with a molecular weight that was ~8-fold higher than that of the native protein. Yet, the ability of VEGF-BD/Cy5 to bind and activate VEGFR-2 was comparable with that of native VEGF (Figs. 4 and 5). Furthermore, VEGF-BD/Cy5 was readily internalized via receptor-mediated endocytosis, and boronated dendrimers were found in a perinuclear region, similar to boronated RGD liposomes (34).

We previously have reported that VEGF-based fusion proteins retain functional activity, even when $NH_2$-terminal extensions of each VEGF subunit were ~3-fold larger than

[6] M.V. Backer, unpublished.

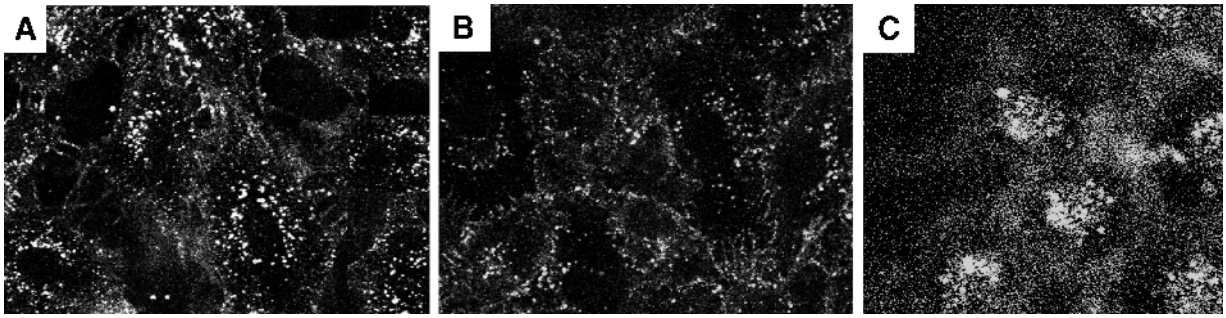


**Figure 4.** VEGF-BD/Cy5 is internalized by PAE/KDR cells via receptor-mediated endocytosis. PAE/KDR exposed to 14 nmol/L VEGF-BD/Cy5 (**A**), mixture of 14 nmol/L VEGF-BD/Cy5 and 1.4 μmol/L VEGF (**B**), or BD/Cy5 at final Cy5 concentration of 20 nmol/L (**C**).

VEGF itself (25, 32). Based on this, we hypothesized that VEGF might serve as a vehicle for targeted delivery of large boron payloads. The results obtained with VEGF-BD/Cy5 strongly support this hypothesis and provide further arguments for the development of VEGF based boron delivery agents. This could be greatly facilitated by using imaging methods for analysis of targeting, biodistribution, and pharmacokinetics. We therefore designed VEGF-BD/Cy5 as a potential ''theranostic,'' a construct that combines potential therapeutic use with an imaging modality (35, 36). The insertion of the near-IR Cy5 dye into the bioconjugate allowed near-IR fluorescent imaging of its uptake in s.c. tumors. Using the 4T1 mouse tumor model, we found that VEGF-BD/Cy5 selectively accumulated in the peripheral areas of growing tumors, where tumor neovascularization was most active (Fig. 5). Importantly, accumulation of VEGF-BD/Cy5 in the tumor neovasculature apparently was not prevented by endogenous tumor-elicited VEGF. These near-IR fluorescent imaging results are consistent with our recent finding that $^{99m}$Tc-labeled VEGF-driven assembled targeting complexes accumulate in s.c. 4T1 tumors displaying a distinctly nonhomogenous intratumoral distribution of the radiolabel (37).

Hypothetically, selective VEGF-BD/Cy5 accumulation in tumors might be due to nonspecific enhancement of permeability/retention mechanisms, known to be involved in the accumulation of macromolecules in tumors (38). However, accumulation of VEGF-BD/Cy5 in tumors seems VEGFR-2 mediated for two reasons. First, untargeted BD/Cy5 did not accumulate in the tumor area (Fig. 5B). Second, pretreatment with the SLT-VEGF fusion toxin produced a 10-fold reduction in VEGF-BD/Cy5 accumulation in the tumor (Fig. 5C–D). As we have recently shown, systemic treatment of 4T1 tumor-bearing mice with SLT-VEGF

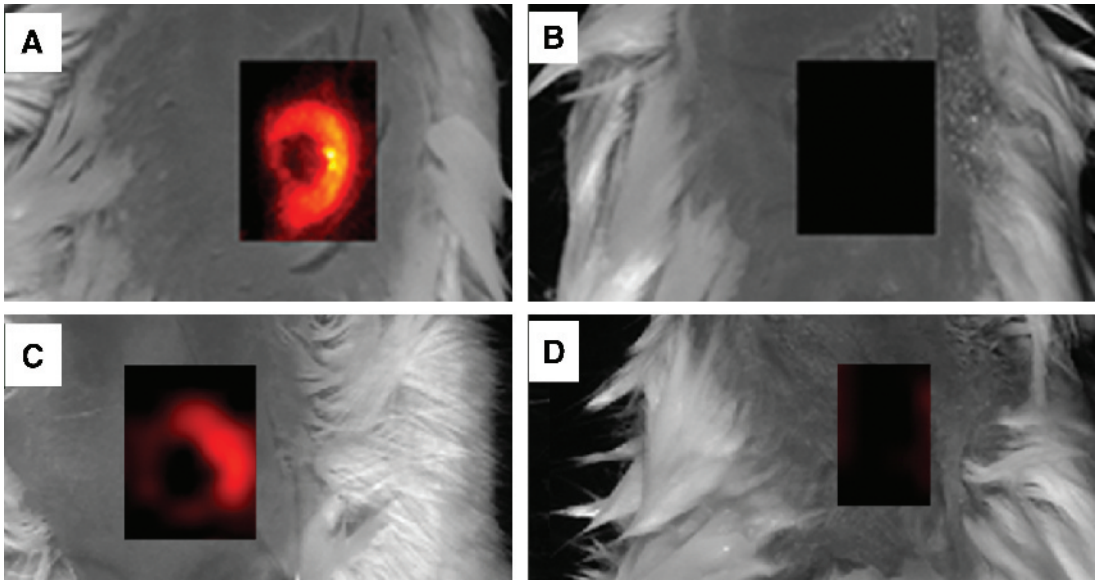


**Figure 5.** VEGF-BD/Cy5 accumulates in specific regions of tumor vasculature. *In vivo* fluorescent imaging of 4T1 tumor-bearing mice after injection of VEGF-BD/Cy5 (**A** and **C**), untargeted BD/Cy5 (**B**), and VEGF-BD/Cy5 in mice pre-treated with SLT-VEGF (**D**). For comparison, pairs of fluorescent images (**A**–**B** and **C**–**D**) were normalized to the same range of intensity, and images from the areas of tumors were superimposed onto visible images of the corresponding mice. After adjusting intensities to a narrow range, fluorescent images (**B**) and (**D**) showed ~10-fold lighter signals than those of images (**A** and **C**). Using Kodak Image Analysis software, relative intensities of fluorescent signal in each of the region of interest was determined versus a similar size and shape region on the back of the same mouse.

selectively eliminated only VEGFR-2-overexpressing cells and did not affect the majority of tumor endothelial cells expressing low to moderate levels of VEGFR-2.[6] Therefore, decreased VEGF-BD/Cy5 accumulation in SLT-VEGF-treated mice cannot be attributed to the reduced tumor vascularity.

The therapeutic use of VEGF-BD/Cy5, or more advanced VEGF-driven boron containing bioconjugates, would depend on their ability to kill endothelial cells in the tumor neovasculature and thereby cause vascular occlusion and ischemic necrosis of the tumor. Experiments are in progress to establish whether a sufficient number of $^{10}B$ atoms can be delivered to tumor endothelial cells to cause tumor cell death following BNCT.

### References


**1.** Barth RF, Coderre JA, Vicente MGH, Blue TE. Boron neutron capture therapy of cancer: current status and future prospects. Clin Cancer Res 2005;11:3987 – 4002.

**2.** Soloway AH, Tjarks W, Barnum BA, et al. The chemistry of neutron capture therapy. Chem Rev 1998;98:1515 – 62.

**3.** Hartman T, Carlsson J. Radiation dose heterogeneity in receptor and antigen mediated boron neutron capture therapy. Radiother Oncol 1994; 31:61 – 75.

**4.** Pouget JP, Mather SJ. General aspects of the cellular response to low- and high-LET radiation. Eur J Nucl Med 2001;28:541 – 61.

**5.** Barth RF, Yang W, Adams DM, et al. Molecular targeting of the epidermal growth factor receptor for neutron capture therapy of gliomas. Cancer Res 2002;62:3159 – 66.

**6.** Barth RF, Wu G, Yang W, et al. Neutron capture therapy of epidermal growth factor positive gliomas using boronated cetuximab (IMC-C225) as a delivery agent. Appl Radiat Isot 2004;61:899 – 903.

**7.** Capala J, Barth RF, Bendayan M, et al. Boronated epidermal growth factor as a potential targeting agent for boron neutron capture therapy of brain tumors. Bioconjugate Chem 1996;7:7 – 15.

**8.** Yang W, Barth RF, Rotaru JH, et al. Boron neutron capture therapy of brain tumors: enhanced survival following intracarotid injection of sodium borocaptate with or without blood-brain barrier disruption. Int J Radiat Oncol 1997;37:663 – 72.

**9.** Yang W, Barth RF, Wu G, et al. Development of a syngeneic rat brain tumor model expressing EGFRvIII and its use for molecular targeting studies with monoclonal antibody L8A4. Clin Cancer Res 2005;11: 341 – 50.

**10.** Yang W, Barth RF, Adams DM, Soloway AH. Intratumoral delivery of boronated epidermal growth factor for neutron capture therapy of brain tumors. Cancer Res 1997;57:4333 – 9.

**11.** Yang W, Barth RF, Wu G, et al. Boronated epidermal growth factor as a delivery agent for neutron capture therapy of EGFR positive gliomas. Appl Radiat Isot 2004;61:981 – 5.

**12.** Gedda L, Olsson P, Ponten J, Carlsson J. Development and *in vitro* studies of epidermal growth factor-dextran conjugates for boron neutron capture therapy. Bioconjugate Chem 1996;7:584 – 91.

**13.** Barth RF, Adams DM, Soloway AH, Alam F, Darby MV. Boronated starburst dendrimer-monoclonal antibody immunoconjugates: evaluation as a potential delivery system for neutron capture therapy. Bioconjugate Chem 1994;5:58 – 66.

**14.** Wu G, Barth RF, Yang W, et al. Site-specific conjugation of boron-containing dendrimers to anti-EGF receptor monoclonal antibody cetuximab (IMC-C225) and its evaluation as a potential delivery agent for neutron capture therapy. Bioconjugate Chem 2004;15:185 – 94.

**15.** Liu L, Barth RF, Adams DM, Soloway AH, Reisfeld RA. Bispecific antibodies as targeting agents for boron neutron capture therapy of brain tumors. J Hematother 1995;4:477 – 83.

**16.** Liu L, Barth RF, Adams DM, Soloway AH, Reisfeld RA. Critical evaluation of bispecific antibodies as targeting agents for boron neutron capture therapy of brain tumors. Anticancer Res 1996;16:2581 – 7.

**17.** Shukla S, Wu G, Chatterjee M, et al. Synthesis and biological evaluation of folate receptor-targeted boronated PAMAM dendrimers as potential agents for neutron capture therapy. Bioconjugate Chem 2003; 14:158 – 67.

**18.** Folkman J. Angiogenesis in cancer, vascular, rheumatoid and other disease. Nat Med 1995;1:27 – 31.

**19.** Veikkola T, Karkkainen M, Claesson-Welsh L, Alitalo K. Regulation of angiogenesis via vascular endothelial growth factor receptors. Cancer Res 2000;60:203 – 12.

**20.** Brown LF, Berse B, Jackman RW, et al. Expression of vascular permeability factor (vascular endothelial growth factor) and its receptors in breast cancer. Hum Pathol 1995;26:86 – 91.

**21.** Couffinhal T, Kearney M, Witzenbichler B, et al. Vascular endothelial growth factor/vascular permeability factor (VEGF/VPF) in normal and artherosclerotic human arteries. Am J Pathol 1997;150:1673 – 85.

**22.** Jackson MW, Roberts JS, Heckford SE, et al. A potential autocrine role for vascular endothelial growth factor in prostate cancer. Cancer Res 2002;62:854 – 9.

**23.** Dev IK, Dornsife RE, Hopper TM, et al. Antitumour efficacy of VEGFR2 tyrosine kinase inhibitor correlates with expression of VEGF and its receptor VEGFR2 in tumor models. Br J Cancer 2004;91:1391 – 8.

**24.** Arora N, Maood R, Zheng T, Cai J, Smith L, Gill PS. Vascular endothelial growth factor chimeric toxin is highly active against endothelial cells. Cancer Res 1999;59:183 – 8.

**25.** Backer MV, Backer JM. Targeting endothelial cells overexpressing VEGFR-2: selective toxicity of Shiga-like toxin-VEGF fusion proteins. Bioconjugate Chem 2001;12:1066 – 73.

**26.** Veenendaal LM, Jin H, Ran S, et al. *In vitro* and *in vivo* studies of a VEGF121/rGelonin chimeric fusion toxin targeting the neovasculature of solid tumors. Proc Natl Acad Sci U S A 2002;99:7866 – 71.

**27.** Alam F, Soloway AH, Barth RF, Mafune N, Adams DM, Knoth WH. Boron neutron capture therapy: linkage of a boronated macromolecule to monoclonal antibodies directed against tumor-associated antigens. J Med Chem 1989;32:2326 – 30.

**28.** Mujumdar RB, Ernst LA, Mujumdar SR, Lewis CJ, Waggoner AS. Cyanine dye labeling reagents: sulfoindocyanine succinimidyl esters. Bioconjugate Chem 1993;4:105 – 11.

**29.** Backer MV, Gaynutdinov TI, Gorshkova II, et al. Humanized docking system for assembly of targeting drug delivery complexes. J Control Release 2003;89:499 – 511.

**30.** Backer MV, Gaynutdinov TI, Aloise R, Przekop K, Backer JM. Engineering S-protein fragments of bovine ribonuclease A for targeted drug delivery. Protein Expr Purif 2002;26:455 – 61.

**31.** Backer MV, Gaynutdinov T, Patel V, Jehning B, Myshkin E, Backer JM. Adapter protein for site-specific conjugation of payloads for targeted drug delivery. Bioconjugate Chem 2004;15:1021 – 9.

**32.** Backer MV, Backer JM. Functionally active VEGF fusion proteins. Protein Expr Purif 2001;23:1 – 7.

**33.** Backer MV, Elliot J, Gaynutdinov TI, Backer JM. Assembly of targeting complexes driven by a single-chain antibody. J Immunol Methods 2004;289:37 – 45.

**34.** Koning GA, Fretz MM, Woroniecka U, Storm G, Krijger GC. Targeting liposomes to tumor endothelial cells for neutron capture therapy. Appl Radiat Isot 2004;61:963 – 7.

**35.** Picard FJ, Bergeron MG. Rapid molecular theranostics in infectious diseases. Drug Discov Today 2002;7:1092 – 101.

**36.** Gumbleton M, Stephesn DJ. Coming out of the dark: the evolving role of fluorescence imaging in drug delivery research. Adv Drug Deliv Rev 2005;57:5 – 15.

**37.** Blankenberg FG, Mandl S, Cao Y-A, et al. Tumor imaging using a standardized radiolabeled adapter protein docked to vascular endothelial growth factor (VEGF). J Nucl Med 2004;45:1373 – 80.

**38.** Maeda H, Wu J, Sawa T, Matsumura Y, Hori KJ. Tumor vascular permeability and the EPR effect in macromolecular therapeutics: a review. J Control Release 2000;65:271 – 84.